Computers and Electronics in Agriculture 211 (2023) 107998

Contents lists available at ScienceDirect

Computers and Electronics in Agriculture

journal homepage: www.elsevier.com/locate/compag

Design, development, and assessment of a High-Throughput Screening (HTS) system for the macroscopic root water uptake modeling

Àngela Puig-Sirera [a,b,e], Lorenzo Bonzi [a,b], Lorenzo Cotrozzi [a,e], Fatma Hamouda [a,b], Alessandra Marchica [c], Giuseppe Provenzano [d,1], Damiano Remorini [a,e], Giovanni Rallo [a,b,e,*]

[a] Department of Agriculture, Food and Environment, Università di Pisa, Via del Borghetto 80, 56124 Pisa, Italy
[b] Agrohydrological Sensing and Modeling Laboratory, Università di Pisa, Via del Borghetto 80, 56124 Pisa, Italy
[c] Center of Plant Sciences, Scuola Supeiore Sant'Anna, Piazza Martiri della Libertà 33, 56127 Pisa, Italy
[d] Department of Agricultural, Food and Forest Sciences, Università degli Studi di Palermo, Viale delle Scienze 12 Ed. 4, 90128 Palermo, Italy
[e] CIRSEC, Centre for Climate Change Impact, Università di Pisa, Via del Borghetto 80, 56124 Pisa, Italy

ARTICLE INFO

Keywords:
Agro-hydrological modeling
High-throughput systems
Root water uptake
Water stress function

ABSTRACT

Climate change is responsible for the increasing frequency and intensity of abiotic stresses generating water scarcity conditions. There is a need to breed plants adapted to future environmental conditions and resistant to water stress. This study presents a High-Throughput Screening (HTS) system for continuously and simultaneously monitoring plant stress response to drought in a semi-controlled environment. The HTS system combines a gravimetric weighing system with soil moisture and atmospheric sensors. In operative terms, the system was tested on the Sage (*Salvia officinalis L.*) under two soil water deficit treatments managed according to a feedback control irrigation scheduling.

The system was able to model the sage water stress function following the root water uptake macroscopic approach. The threshold of soil water status below which crop water stress occurred was also identified. The gravimetric-based daily evapotranspiration (ET_a) and the time domain reflectometry (TDR)-based root water-uptake (*RWU*) rates showed a high correlation during the drying when the evaporation flux is minimal. Moreover, the effects of soil bulk density on the root density and the plant biomass were evaluated, indicating the importance of carrying out a homogeneous procedure of the pot-filling process.

1. Introduction

Global climate change and the decreasing water availability for agriculture have driven the research to study the crop physiological traits and to develop cultivars more tolerant to drought stress.

The main difficulties in researching drought-adapted cultivars are associated with the complex nature of mechanisms characterizing the crop tolerance to abiotic stresses, the instability and uncertainty of environmental conditions, the lack of well-defined stress scenarios, the identification of trait phenotypes tolerant to drought conditions (Gosa, Lupo and Moshelion, 2019). The latter is essential to study as the plant's physiological traits describe the plant regulation mechanisms that control the plant's stress response, productivity, and resilience to unfavourable conditions (Joshi et al., 2017; Stahl, Wittkop, and Snowdon, 2020).

High-throughput screening (HTS) systems are gaining relevance in research worldwide. Using these platforms to study the plant response to abiotic-induced stresses can be a solution to face climate change and increased water demand in agriculture and to foster "climate-ready crops" that enhance the resilience of agroecosystems (Negin and Moshelion, 2016).

The HTS systems are non-destructive and non-invasive tools that continuously detect crop response to different soil and atmospheric conditions. In this context, the accuracy of HTS allows the detection and comparison of small changes in specific eco-physiological behaviours associated with the plant response to environmental constraints, such as water deficit conditions (Gosa, Lupo, and Moshielion, 2019; Walter et al., 2015). In this way, the HTS systems can identify plants characterised by a high recovery rate after stress regaining their whole-plant pre-stress capabilities (e.g., photosynthesis, transpiration) early after

* Corresponding author.
E-mail address: giovanni.rallo@unipi.it (G. Rallo).
[1] Deceased December 1, 2022.

https://doi.org/10.1016/j.compag.2023.107998
Received 20 December 2022; Received in revised form 15 June 2023; Accepted 15 June 2023
Available online 4 July 2023

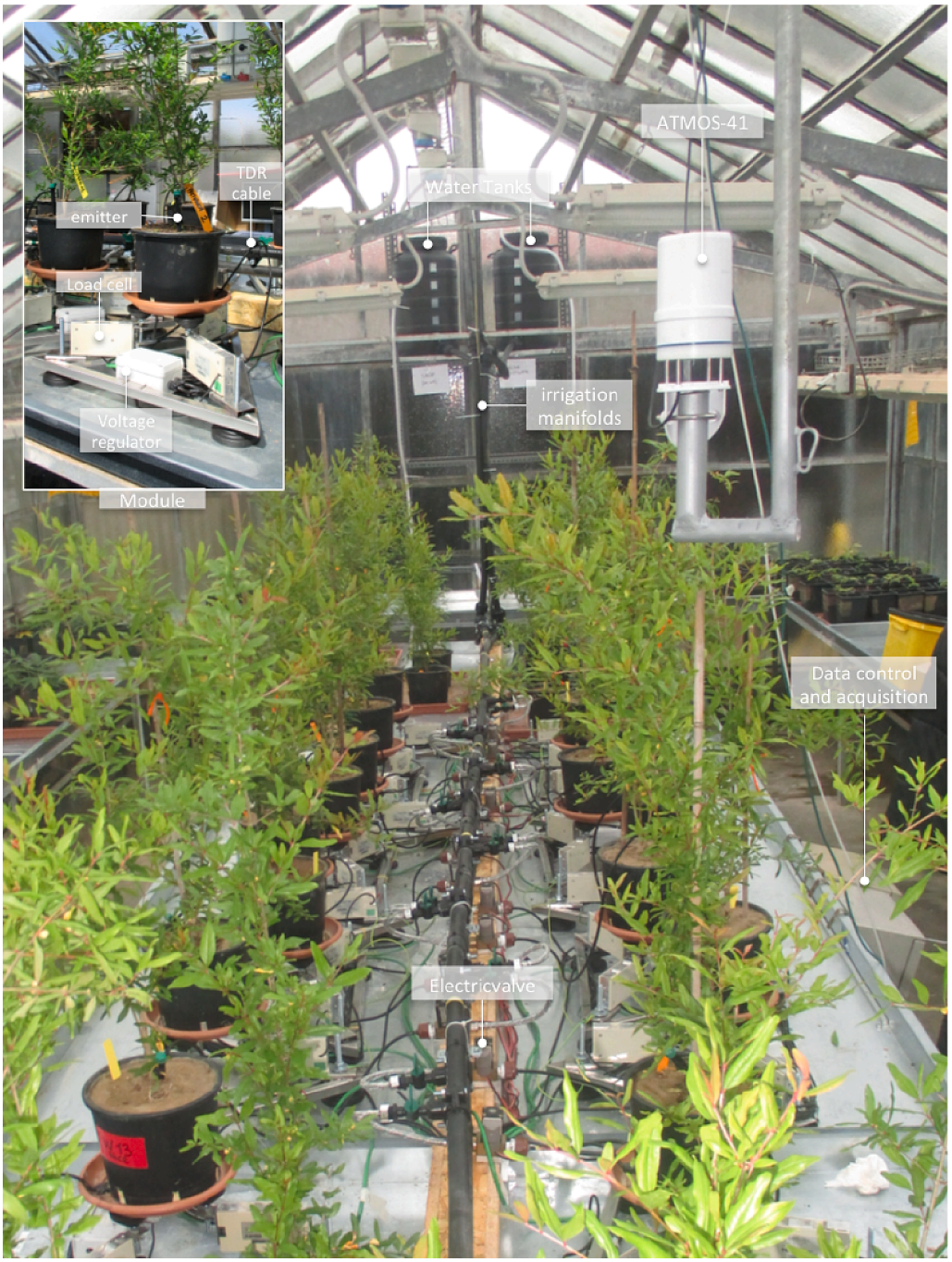

Fig. 1. Panoramic image of the HTS system. In detail, the main parts of a single module are shown.

the stress has finished (Walter et al., 2015).

The most used HTS systems are in plant containers (Jiménez-Carvajal et al., 2017) and combine image analysis, 3D-scanning, and lysimetric facilities integrated with contact and proximity sensors (Dalal et al., 2020). Moreover, the inclusion of automatic irrigation systems in each plant container enables the precise monitoring of soil water content and hence, the definition of drought stress scenarios (Stahl et al., 2020).

Even if the available HTS systems have produced advancements in the quality of data acquisition and pre-processing, the existing HTS types do not often account for some plant feedback processes, such as the impacts of root water uptake (*RWU)* variability and the pot scale effect to upscale the results to field environments (Stahl et al., 2020). The former aspect is essential as it influences the water stress accumulation by the plant, which may affect the final product (Puig-Sirera et al., 2021). However, to the best of our knowledge, the possibility of using the soil moisture sensor-based *RWU* indicator to estimate the ET_a fluxes has been only qualitatively studied by Halperin et al. (2017) and Ardakani et al. (2014). The second plant feedback process considers extrapolating the results of controlled greenhouse pot-based experiments to actual field conditions, which may need to be more representative. Nonetheless, the HTS system allows a fast and prompt assessment of the functional soil–plant-atmosphere interactions traits, which is difficult to achieve in open-field experiments.

From an agro-hydrological point of view, the measured gravimetric variations of soil water content can be converted into *RWU* to identify the evapotranspiration (ET_a) and transpiration (T) fluxes. Moreover, these data can be used to fit a macroscopic *RWU* model able to detect the soil moisture critical threshold, below which crop T starts to reduce

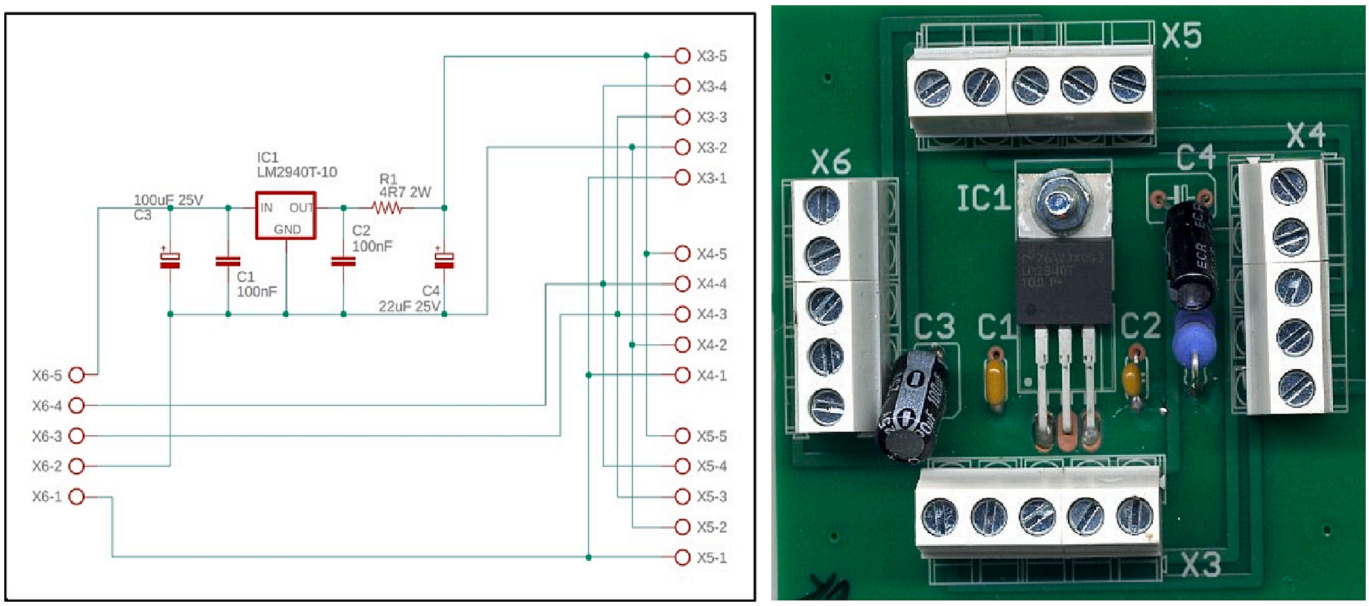

Fig. 2. Wiring diagram and detail of the 4-way voltage regulator/stabilizer. Pin 1: Shield; Pin 2: GND; Pin 3: Signal; Pin 4: Signal; Pin 5: Power supply.

since the soil water content is a limiting factor. These phenotypic data should be traced precisely and efficiently during the whole crop cycle to predict the specific plant response to soil water stress, which represents the most common drought-resilient trait (de Souza et al., 2014; Rallo et al., 2017; Sadras and Milroy, 1996; Walter et al., 2015).

Sinclair (2017) described the different phases in which the relationship between the *T* rate and the soil water status, expressed as the fraction of transpirable soil water (*FTSW)*, can be divided. In phase I, there is no limitation for the *T* rate because soil water is readily available to the plant. In contrast, in phase II, in the range below a particular value of *FTSW* and 0, the *T* rates decrease until phase III starts. The plant closes the stomata to avoid further water loss and enters survival mode at this stage. The author defined the threshold of soil water status as a critical parameter to identify the sensitivity of the plant to the soil water deficit. Thus, each plant and species would initiate the stomatal closure at certain soil water status, which regulates the plant's physiological activity during the period of water deficit.

However, different studies have highlighted the spatial heterogeneity of soil water content and the inaccuracies derived when defining the plant response to water stress only based on a soil water status threshold (Halperin et al., 2017; Sadras and Milroy, 1996). The heterogeneous patterns of soil moisture depend on many factors, such as root spatial variability, soil physical properties, irrigation depth, quantity and frequency of irrigation, and the type of water distribution system. Specifically, Guswa et al. (2004) highlighted the impact of the spatial distribution of soil moisture in the root volume on the total root water uptake. The crop water stress response to soil water status is not linear and not uniquely associated with each crop species but depends on the degree of wetting uniformity in the root zone.

Evaluating crop drought traits under controlled experiments allows adjusting the water limiting factor and standardising the boundary conditions (i.e. atmosphere evaporative demand) to test the scientific hypotheses under investigation. However, experiments in greenhouses with individual pots must be upscaled to field conditions. The complex interactions among the variables involved in the crop response to drought make the transferability of results from greenhouse to field conditions challenging, mainly due to pot effects: insufficient soil volumes that could hold back the potential root growth, the influence of the root-shoot ratio, the increase in soil temperature, as well as the soil salinity, the variations of soil moisture and the higher irrigation requirements due to increased root extraction (Atkinson et al., 2019; Stahl et al., 2020).

A critical point for any HTS system is the need for equal growing conditions among the plant containers to compare data from different plant species and genotypes. The soil containers must be homogeneous in bulk density and standardized methods must be adopted to fill the soil containers and avoid dissimilar soil compaction (Stahl et al., 2020).

Considering the importance of quantitative analysis to assess the implications of plant water stress on crop yield and quality, there is the need to dispose of accurate and non-disruptive methods to measure actual evapotranspiration (ET_a) and to help farmers with greenhouse management to improve the resource use efficiency.

The general objective of this study was to design, develop, and assess High-Throughput Screening (HTS) system for the macroscopic root water uptake modelling by integrating atmometric, gravimetric and embedded TDR (Time Domain Reflectometry) probes in the pot. The system was assessed on sage (*Salvia officinalis* L.), an aromatic crop cultivated mainly for its essential biological properties and high tolerance level against abiotic stresses (Marchica et al., 2019). Moreover, specific objectives were i) to develop an accurate and user-friendly HTS system under controlled conditions; ii) to investigate the water stress function and the hidden water stress resilient features for sage; iii) to compare the gravimetric-based and the soil moisture-based approaches to measure the ET_a fluxes and iv) to analyze the effects on the soil–plant system variability (I.e., the soil bulk density) that could be created during the experimental set-up.

2. Materials and methods

2.1. Design of the HTS system

The HTS system was located at the experimental station of San Piero a Grado of the Department of Agriculture, Food and Environment (DAFE) of the University of Pisa (Italy; 43°40′48″ N, 10°20′46″ E, 2 m a.s.l.), and was designed by the AgroHydrological Sensing and Modeling (AgrHySMo) laboratory of DAFE.

Structurally, each of the 16 modules of the HTS system consists of three hardware segments for the high-frequency detection of the agro-meteorological forcing variables (i.e., atmometry), the weights (i.e., gravimetry), and the soil water content (i.e., time domain reflectometry, TDR) of sixteen pots growth. Moreover, a cybernetic platform allows the analysis in real-time and data download.

Table 1
Calibration equation parameter, coefficient of determination, and the hysteresis error of each module implemented in the HTS system.

ID	Offset (g)	Slope (g/mV)	Coeff. of determination, R^2	Hysteresis (% of R.O.)
POT 01	−5c931.585	448.279	0.9997	0.016
POT 02	−3746.104	434.984	0.9997	0.012
POT 03	715.716	441.237	0.9996	0.017
POT 04	923.238	436.386	0.9996	0.017
POT 05	−384.336	435.832	0.9997	0.011
POT 06	7838.760	483.750	0.9991	0.011
POT 07	5361.137	449.036	1.0000	0.013
POT 08	−889.946	437.254	0.9910	0.013
POT 09	−952.042	447.000	1.0000	0.011
POT 10	1706.000	451.000	1.0000	0.010
POT 11	−548.428	448.535	1.0000	0.010
POT 12	−1013.069	441.893	1.0000	0.009
POT 13	−10210.400	433.337	1.0000	0.010
POT 14	−8224.000	432.260	0.9996	0.013
POT 15	−4447.085	437.540	0.9996	0.014
POT 16	−1132.007	435.780	1.0000	0.010

An automated micro-irrigation system was designed to manage the water of every single module by following a feedback control irrigation scheduling protocol. The three monitoring segments and the irrigation system control were implemented in an algorithm written in CRBasic programming language. Fig. 1 shows a panoramic image of the HTS system.

2.1.1. Weighing and soil water content measurement of the single module

The gravimetric segment uses a high-resolution load cell (LC) to weigh (*W*) each module. For each module, three LCs model U2D1-3 K (NMB-Minebea Ltd, Bangkok, Thailand) were fixed over a steel beam triangle and allowed to reach a maximum load capacity of 9 Kg.

To this aim, a voltage regulator/stabilizer circuit was designed and built to power the three load cells per module with the same constant voltage of 10 Volts. Fig. 2 shows the wiring diagram and the photo of the voltage regulator/stabilizer, consisting of a low-dropout regulator (LDO), which allows setting the constant excitation voltage of the cells.

Every single module of the gravimetric segment was preliminarily calibrated based on standard metrology protocol (IMCCP, 2011). According to the protocol, the three-run method was followed after the warmup and preloading periods. Operatively, we record and analyse five substantially equally spaced loads, covering the weighing range of the load cell. Finally, the calibration equation's fitting parameters (offset and slope) and the hysteresis have been quantified.

Concerning the hysteresis, the relative error has been calculated by normalising, for the rated output (R.O.), the algebraic difference between output at 50% load descending from the maximum load and output at 50% load ascending from the minimum load. Table 1 shows the parameters of the calibration equation, the coefficient of determination, and the hysteresis error of each module implemented in the HTS system.

According to a voltage supply of 10 V, the average calibration slope was equal to 44.3 g mV^{-1} V^{-1}. Therefore, considering the CR1000 datalogger A/D resolution equal to 0.067 mV $count^{-1}$ (CR1000-Measurement and Control System), the LC resolution was estimated to equal 2.95 g $count^{-1}$ V^{-1}, according to the procedure proposed in Evett et al. (2009).

Fig. 3. TDR probes integrated into the pot (left) and the complete module (right) of the HTS system.

The TDR probe, integrated into each pot, was designed based on a multi-wire configuration (hexagonal geometry) to maintain the electrical field inside the soil volume (Fig. 3). In particular, the soil monolith was 130 mm in height. The active part of the TDR probe covered a profile of 125 mm, its head fixed at the bottom of the pot.

To guarantee a homogeneous load distribution over the three load-cells, we use a rigid plant saucer opportunely holed to fast remove any excess water drained from the pot.

2.1.2. Environmental data and control

The HTS system was installed in a semi-controlled environment (double-glazed greenhouse), where it was possible to control the solar radiation through shading sheets, the air temperature, and relative humidity through a fan and active cooling (i.e., evaporative cooling pad) system. The greenhouse, oriented in the East-West direction, is 15 m in length, 8 m in width, and 3 m high.

The segment to monitor the climate variables consisted of a standard agrometeorological station, model ATMOS-41, connected to a data logger model ED50 of the METER Group (Pullman, WA, USA). The weather station measured atmospheric pressure (*Pa*), air temperature (T_a), relative humidity (*RH*), vapour pressure deficit (*VPN*), global solar radiation (*Rg*), wind speed (u_2), and wind direction (v_{dir}). The climate forcings were acquired every 15 min and paired with the gravimetric and TDR acquisitions. The meteorological measurements allowed the calculation of reference evapotranspiration (ET_0) using the Penman-Monteith model proposed by Allen et al. (1998).

2.1.3. Data acquisition, programming, and system control

Data acquisition and the control system used Campbell Scientific Inc. (Loughborough, UK) technologies. A data logger CR1000 implemented a TDR200 with two levels of multiplexers (model SDM80X) and 16 TDR probes. The CR1000 also managed a multiplexer for differential voltage (DiffVolt) channels (model AM16/32), used for the load cells data acquisition, and a relay controller (model SDM16AC) to open and close the electric irrigation valves.

An AC/12 VDC transformer supplies power to the datalogger and AC/24 VAC through a terminal strip for electric valves. Annexe 1 shows the CAD scheme of the system with highlighted the main wiring among the hardware components.

The TDR segment was programmed to acquire a 251-point waveform (WF) in each module every 15 min for 16 WFs. A specific CRBasic instruction allowed computing the probe bulk length used to calculate the soil dielectric permittivity and the volumetric soil water content (θ_i)

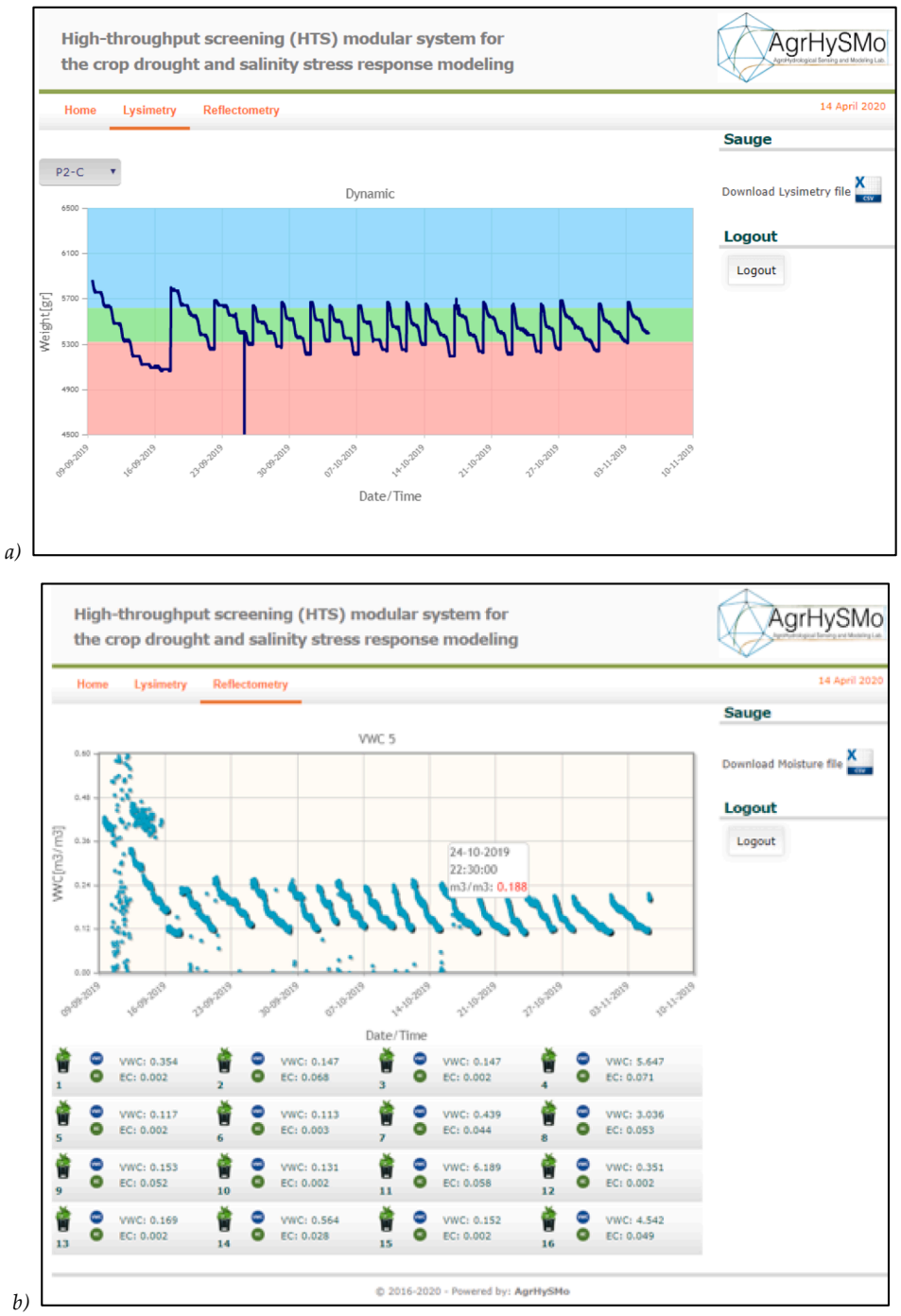

Fig. 4. a, b screenshot of the cybernetic platform used for data display.

according to the universal equation proposed by Topp et al. (1980).

The load cell data were acquired using the DiffVolt command, according to the specific voltage range (±2500 mV) and the equation parameters shown in Table 1.

Complete irrigation automation follows the feedback control approach based on a critical weight and soil water content threshold. Soil moisture thresholds can be obtained using the method of Polak and Wallach (2001) or Thompson et al. (2007). According to this procedure, all the pots must be saturated at the beginning of the experiment and then monitored at high frequency during the drying process until the θ_i is constant. Initially, a rapid i decrease is observed, mainly due to the free drainage process (FD). Then, a significantly slower extinction occurred due to the combination of drainage (D) and root water uptake (RWU) processes. Finally, when the total soil water potential gradients become negligible, the drying process's dynamics only depend on RWU. The points obtained by intersecting the tangent lines characterizing the three hydrological processes allowed identifying the soil field capacity (θ_{fc}) and the critical water content (θ^*). The soil wilting point (θ_{min}) was assumed to correspond to the minimum value measured during the investigated period (Pellegrino et al., 2006). At the service of the HTS system, a web platform has been created to view and download the data, available at https://www.agrhysmo.agr.unipi.it in the Research & 3rd Mission (Account: Guest; Password: Guest) section.

The data acquired and stored in the CR1000 Data Logger (CR1000 Measurement and Control, 2013) are sent via the NL-121 interface of the *.csv database via FTP protocol through the Internet to the server. The

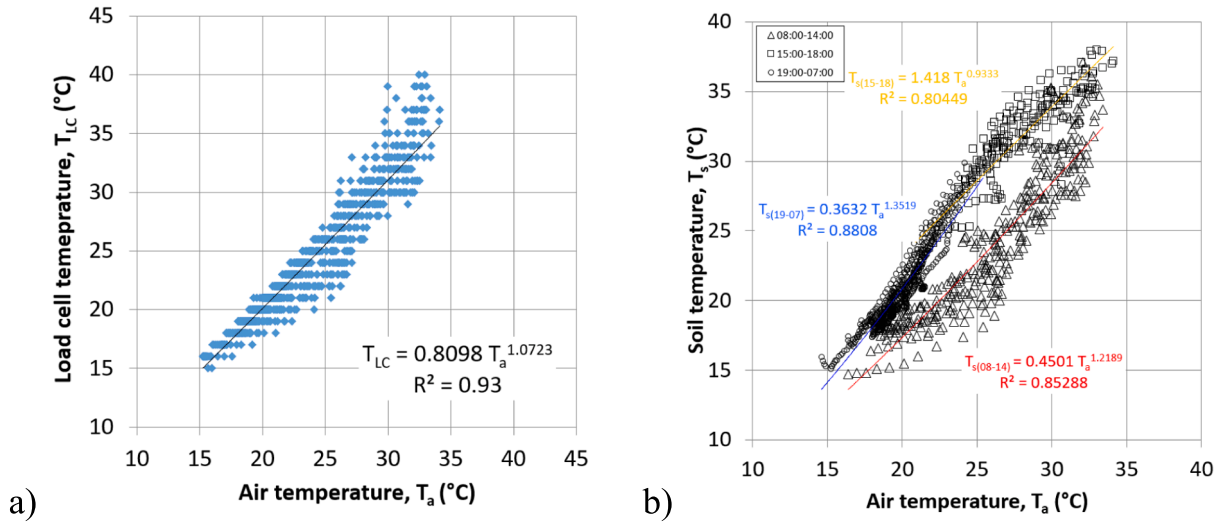

Fig. 5. a) linear regression between load cell, T_{LC}, and air temperature, T_a; b) soil temperature, T_s, and air temperature, T_a, during the three circadian sub-periods in which the daily hours were divided.

server consists of a Virtual Machine (authorized by the University of Pisa) on which the Linux operating system of the Debian 8 release (free software) has been installed. Specifically, the FTP, Apache2 (for HTTP support), and PHP modules have been installed and configured.

The architecture has been implemented on a client–server paradigm: Campbell CR1000, and the web users are the clients. The data, sent regularly by the CR1000, are stored in the server storage in a private area on files in "append" mode to preserve the previous ones.

Each web page plays a specific role, mainly showing the user the data transmitted by the CR1000 and making them accessible using graphs with zoom functionalities and dedicated tooltips. The download of the data, which will be suitably filtered according to the needs, is foreseen in "*.csv" format readable by text application and Excel.

The user interface is simple and intuitive: the home page offers a summary of the internal functions of the site/program, and the menu is limited to the display of the logical operation scheme. On the right side, we have a contextual area where the user finds the section for private access through username and password. Once the user can access the menu, they select the project; then the gravimetry and reflectometry data sections are available. Regarding the main gravimetric and reflectometric data encoding, a synoptic screen allows the user to graph the desired variable over time and for each module. For example, the user can display the dynamic of every single module's weight (Fig. 4a) and volumetric water content, VWC (Fig. 4b). The graph can display three coloured bands, red for values below the minimum irrigation threshold, blue above the maximum limit (e.g., field capacity), and green within the optimal condition. The reflectometry data, further the VWC, can release the soil bulk electrical conductivity, EC.

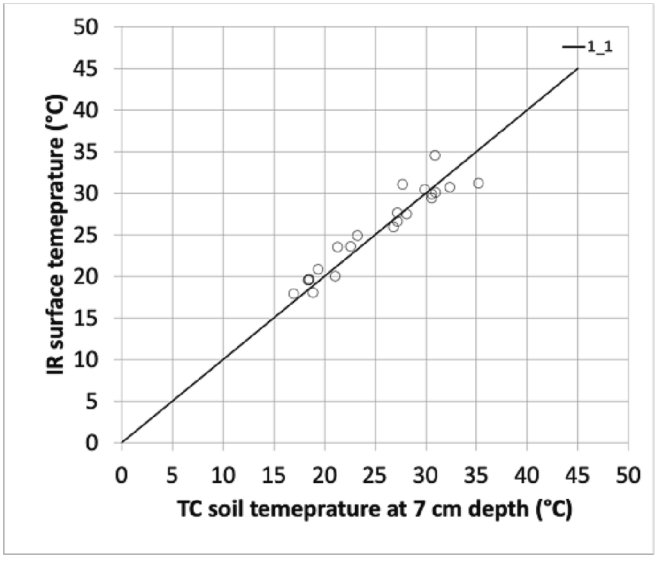

Fig. 6. Comparison between soil temperature measure at 7 cm depth and surface IR.

2.2. Data processing and analysis

Once the values of θ_{fc} and θ_{min} were determined, it was possible to evaluate the fraction of water available for transpiration (*FTSW*) (Sinclair and Ludlow, 1986) corresponding to every actual soil water content (θ_i) used to quantify the soil water status conditions:

$$FTSW = \left(\frac{\theta_i - \theta_{min}}{\theta_{fc} - \theta_{min}}\right) \quad (1)$$

Actual evapotranspiration (ET_a) released by each module of the system was determined using a differential analysis (e.g., finite differences) based on the series of pot weights, W [g], acquired with the frequency (k) of 15 min. The weight loss between two consecutive weightings (k = 15 min), was equal to the crop evapotranspiration including the instantaneous irrigation amount (I_k) and assuming the absence of biomass accumulation and drainage, during short and soil drying periods respectively, was calculated as:

$$ET_a = -\left[\frac{dW}{dt}\right]_k \approx I_k - \frac{W_k - W_{k-1}}{t_k - t_{k-1}} \quad (2)$$

The 24-hour integral of eq. (2) returned the daily amount of actual evapotranspiration.

The *RWU* was as well determined by finite element analysis of the soil moisture values, θ_k, by inverting:

$$-\frac{\theta_k - \theta_{k-1}}{t_k - t_{k-1}} V_s = I_k - E_k(\theta) - RWU_k(\theta) - D_k(\theta) \quad (3)$$

where I_k is the irrigation rate, $E_k(\theta)$ is the soil evaporation, $D_k(\theta)$ is the drainage and V_s is the volume of the soil in the pot.

Assuming the absence of free drainage and soil drying period, the 24-h integral of eq. (3) allowed estimating the daily amount of root water uptake, which included the evaporation term.

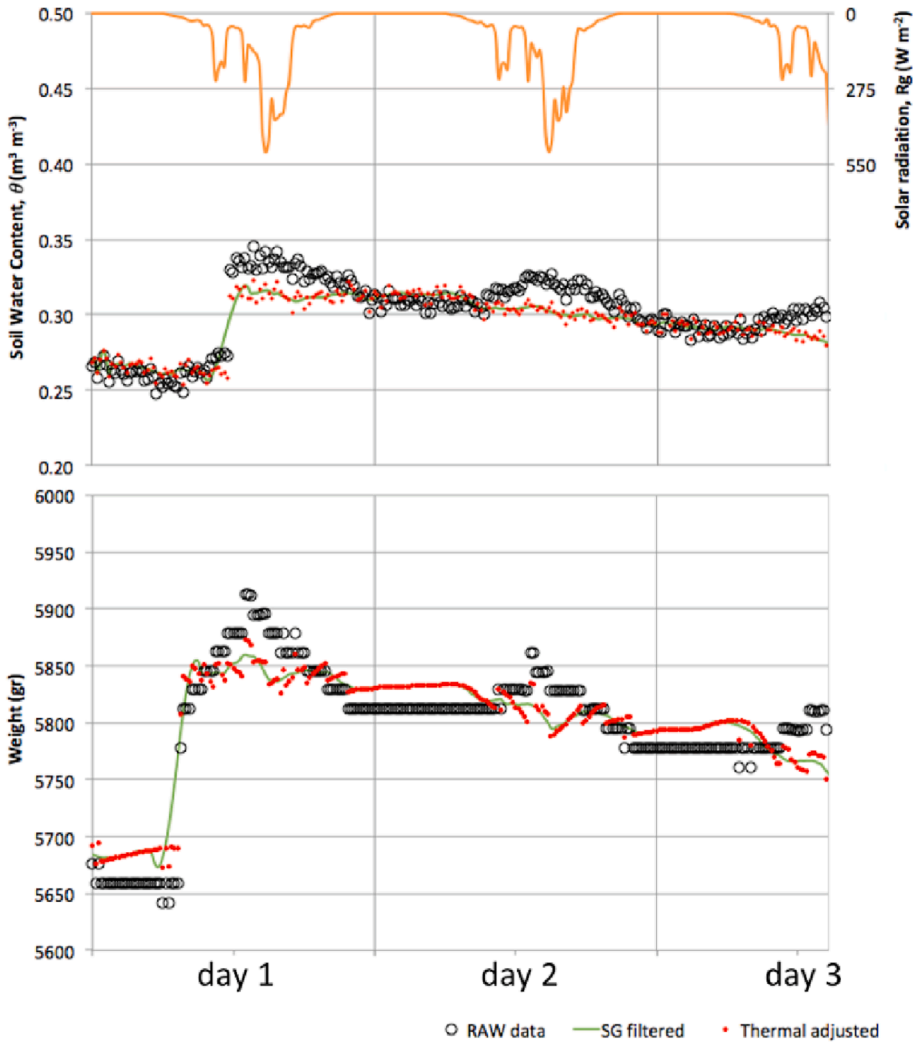

Fig. 7. Raw, thermal drift adjusted, and smoothing processed data of hourly signals collected for three consecutive days of the experimental period.

In line with Xu et al. (2015) which used the vapour pressure deficit (VPD) to normalised ET_a, the relative evapotranspiration *(RET)* was obtained by normalizing the daily ET_a for the corresponding value of the atmospheric water demand (ET_0). The root water uptake model (i.e water stress function, WSF), describing the relationship between *RET* and *FTSW*, was represented through the logistic model:

$$RET = \frac{a}{1 + b\, e^{-c\, FTSW}} \tag{4}$$

where *a, b* and *c* are the shape parameters of the model.

Considering that the response of the load cells and the TDR probes depended on air and soil temperatures, it was preliminarily necessary to correct both sensors' outputs to account for the observed thermal drifts. To this aim, a contact thermocouple CS240 Pt-1000 (Campbell Scientific, UK) was installed on a representative load cell to measure the temperature of the aluminium body. To obtain the correction factor to be applied on each load cell, the potential regression between the load cell temperature, T_{LC}, and the corresponding air temperature, T_a, was used (Fig. 5a).

Similarly, a PT100 thermocouple (Italcoppie, Italy) was installed in a representative soil monolith to measure the soil temperature, T_s. The PT100 was installed in the middle plane of the pot at about 7 cm depth. Periodically comparison with surface IR temperature ensured that the 7 cm depth installation was representative to measure the monolith T° (Fig. 6).

Comparing T_s with the corresponding air temperature, T_a, (Fig. 5b) it was possible to observe three transfer functions, $T_s = f(T_a$; circadian subperiod), valid in the different sub-periods in which the daily hours were divided (08:00–14:00, 15:00–18:00 and 19:00–07:00 Central European Time, CET).

The mathematical models used to remove the thermal effect on the measurements of weight and soil moisture followed those proposed by Minjiao et al. (2015):

$$\chi_{adj} = \chi_i \frac{1 - \frac{a(T_i - T_{ref})}{2}}{1 + \frac{a(T_i - T_{ref})}{2}} \tag{5}$$

where χ_{adj} is the adjusted values of the measured data, T_{ref} is the reference temperature and α is a coefficient. Respectively for the TDR and Load-cell data, *Tref* were 20 °C and 24 °C, whereas α were fixed at 0.0081 $°C^{-1}$ and 0.0015 $°C^{-1}$.

The data sets corrected for the thermal drift were further improved by a smoothing process, which was performed using a 4th order polynomial function (Savitzky and Golay, 1964) on frame lengths equal to 17 points, for the weight, and 9 points for the soil water content variables. Fig. 7 shows the data quality improvemenafter applying the signal adjustment procedure based on the thermal drift and the smoothing process on the raw hourly data acquired with the TDR-based soil water contents and the LC-based system for three consecutive days of the experimental period.

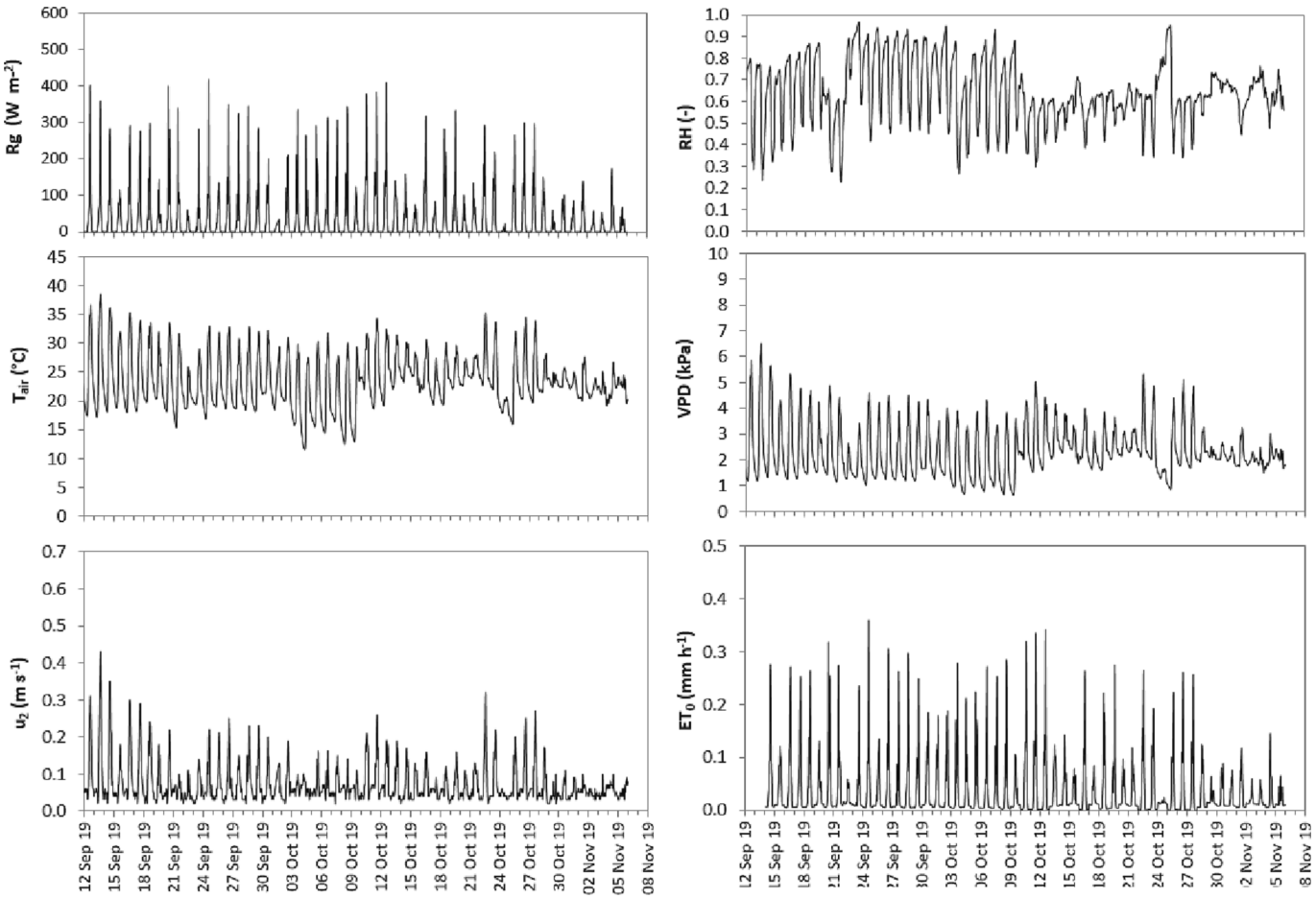

Fig. 8. Trend of agrometeorological variables measured during the experimental period (from 12 September 2019 to 5 November 2019).

2.2.1. Statistical analysis

The statistical analysis was done using JMP Statistical Discovery (JMP© 2023 SAS Institute Inc., Cary, NC, 1989–2023). The distribution frequency of the RWU and ET_a dataset was studied according to the Shapiro-Wilk goodness of fit test to examine if the variables were normally distributed. The No-Parametric Mann-Whitney test (Sheskin, 2007) was used to verify the difference between the methods to calculate water fluxes.

2.3. Assessment of the system for the determination of the root water uptake function

The system was assessed with sage (*Salvia officinalis* L.), an aromatic crop largely cultivated for its essential biological properties and high tolerance level against abiotic stresses (Marchica et al., 2019), cultivated in pots under greenhouse conditions.

The pots were filled with sandy soil and included 4-month-old sage seedlings (around 20 cm tall, selected for uniformity in size).

The plants were developed under natural radiative and wind speed conditions during the initial crop growth phases. Then, they were moved into the greenhouse where the experiment was carried out from 12th September to 5th November 2019.

Eight modules of the HTS system were maintained under soil water deficit (DI) conditions (SAGE-DI) by keeping the soil water content below the critical point. In contrast, the other eight modules of the HTS system (SAGE-FI) were maintained under full irrigation (FI), in the range of soil water contents between the field capacity and the critical point.

Therefore, the irrigation management followed a feedback control protocol, which allowed to identify the irrigation timing (watering start/end) based on two thresholds of θ. (Details on setting and individuating the irrigation thresholds are explained in section 2.1.3).

2.3.1. Crop eco-physiological and biometric measurements

Midday stem water potential (MSWP) was measured four times during the experimental trial by using the Scholander pressure chamber (PMS Model 600, Albany, OR, USA) and the protocol proposed by Turner and Jarvis (1982). Four fully expanded leaves were selected at midday for each treatment and covered with foil-faced bags at least 30 min before measurements. The four measurement days of *MSWP* were distributed weekly during the last month of the trial.

At the end of the experiment, the plant height (*H*) was measured with a rigid tape. The total root weight density (*RWD*), which refers to the root dry weight per unit of soil volume, was finally determined by extracting the roots from the soil following the protocol proposed by Böhm, 1979. The whole soil volume was washed with distilled water, and the extracted root samples were oven-dried at 80 °C until a constant weight was reached and root dry weight was evaluated. At the same time, the dry weight of the epigeal parts of the plant (leaves and roots) was also determined, always after oven-drying at 80 °C until a constant weight was reached.

3. Results and discussion

3.1. Agro-meteorological characteristics

Fig. 8 shows the dynamics of daily standard agrometeorological variables acquired during the experimental period (from 12 September to 5 November 2019) by the weather station installed in the greenhouse.

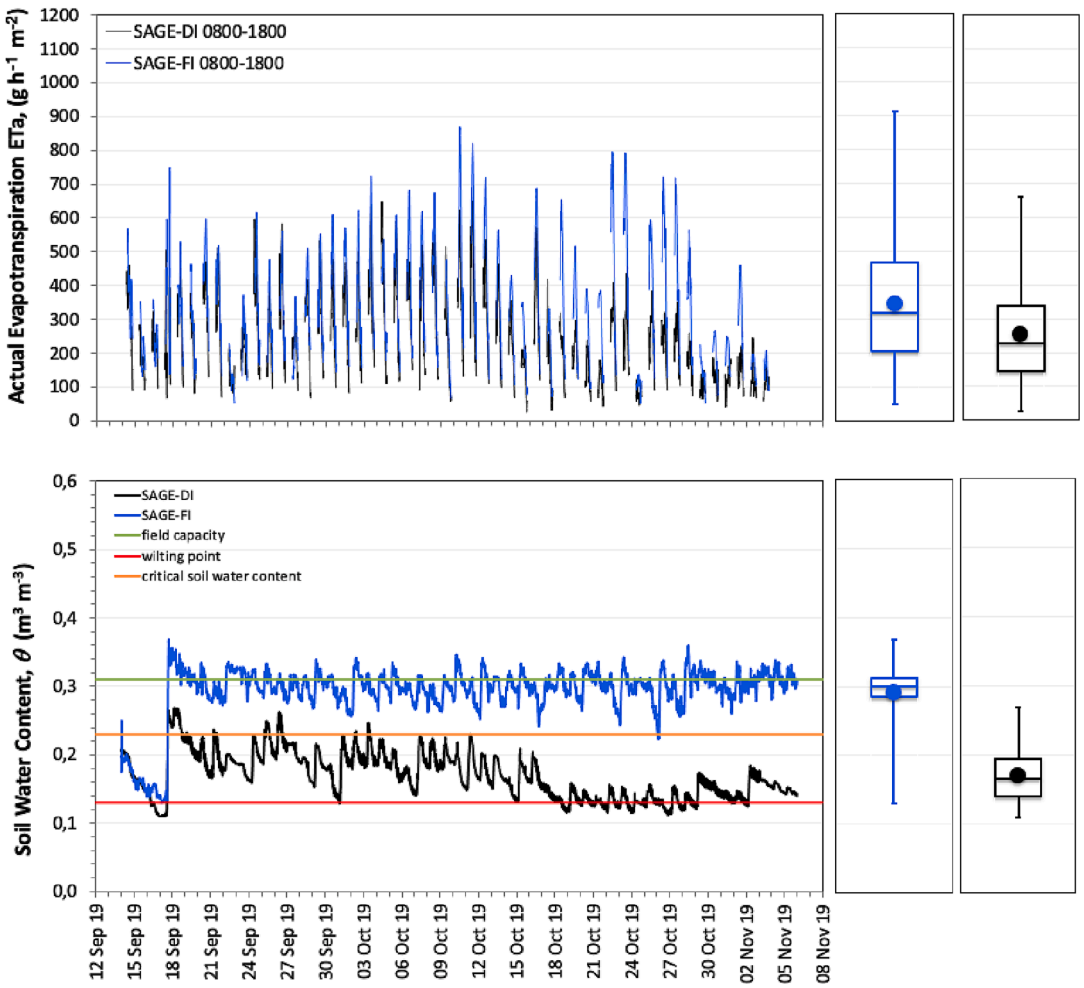

Fig. 9. Temporal dynamic of a) hourly actual evapotranspiration (ET_a) and b) soil water content (q) obtained for the deficit (SAGE-DI) and the full (SAGE-FI) irrigation treatments. The boxplots corresponding to the two treatments are also shown on the right side of the figure.

To avoid heat stress, the air temperature inside the greenhouse was always maintained below 35 °C using a fan system. During the experimental period, there was a specific variability in the daily dynamics of the agrometeorological variables. The values of hourly *Rg* were characterized by a wide range of peaks, from 400 W m^{-2} to 70 W m^{-2} at the beginning and end of the experimental period, respectively, with a decreasing trend during the last month of observation. Similarly, the maximum values of hourly *RH, T_a, VPD,* and u_2 showed decreasing trends from the end of September to November. Consequently, the distribution of hourly reference evapotranspiration, ET_0, showed the highest peak of 0.37 mm h^{-1} in September, whereas the lowest of 0.05 mm h^{-1} was recorded in November.

3.2. Preprocessing of the crop and soil water status data series

Fig. 9a, b shows the temporal dynamic (k = 15 min) of the average soil water content (θ) and hourly actual evapotranspiration (ET_a) acquired during the experimental period for the eight modules of each treatment. The corresponding boxplots for each data series are also shown on the right side of the figure. The ET_a series only includes the daily period from 08:00 to 18:00 (CET). Regarding the instantaneous ET_a fluxes [g h^{-1} m^{-2}], the SAGE-DI treatment showed lower average intensity than the SAGE-FI treatment, with more marked differences around midday. According to the boxplot encoding, the hourly ET_a series for both treatments resulted strongly variable, as indicated by the error bars. Even if the dynamic of soil water content showed a robust intra-treatment variability, two separated soil water status regimes have been established. Therefore, the adopted irrigation protocol allowed us to maintain the average soil water content θ in the pre-defined ranges (i.e., between θ_{fc} and θ^* for SAGE-FI and from θ^* to θ_{min} for the SAGE-DI treatment).

Fig. 10 shows the means and standard deviations of the cumulative ET_a and irrigation amount measured during the study period for both treatments. Each value was calculated as the average of the eight plants included in the treatment.

The total amount of supplied irrigation was 2200 and 1100 g for the SAGE-FI and SAGE-DI treatments, respectively. Consequently, the cumulative ET_a of 1836 g and 1437 g was estimated for the SAGE-FI and SAGE-DI treatments, respectively.

The variability observed in the water fluxes (irrigation amount and ET_a) could be associated with the variability of θ occurring among the treatments. Consequently, the intra-treatment θ variability has caused a phase shift in irrigation timing among different plants of the same treatment because the irrigation timing was based on the soil water status.

3.3. Soil-plant water relations and root water uptake modeling

Fig. 11 a and b show the correlation between the actual daily evapotranspiration (ET_a) and the corresponding root water uptake (*RWU*) derived with eqs. (2) and (3), respectively, during the drying periods for both irrigation treatments. Moreover, the Figures depict the frequency distribution data and the statistical parameters to test the normality of the distribution. A high correlation (R^2 = 0.77, p-value <

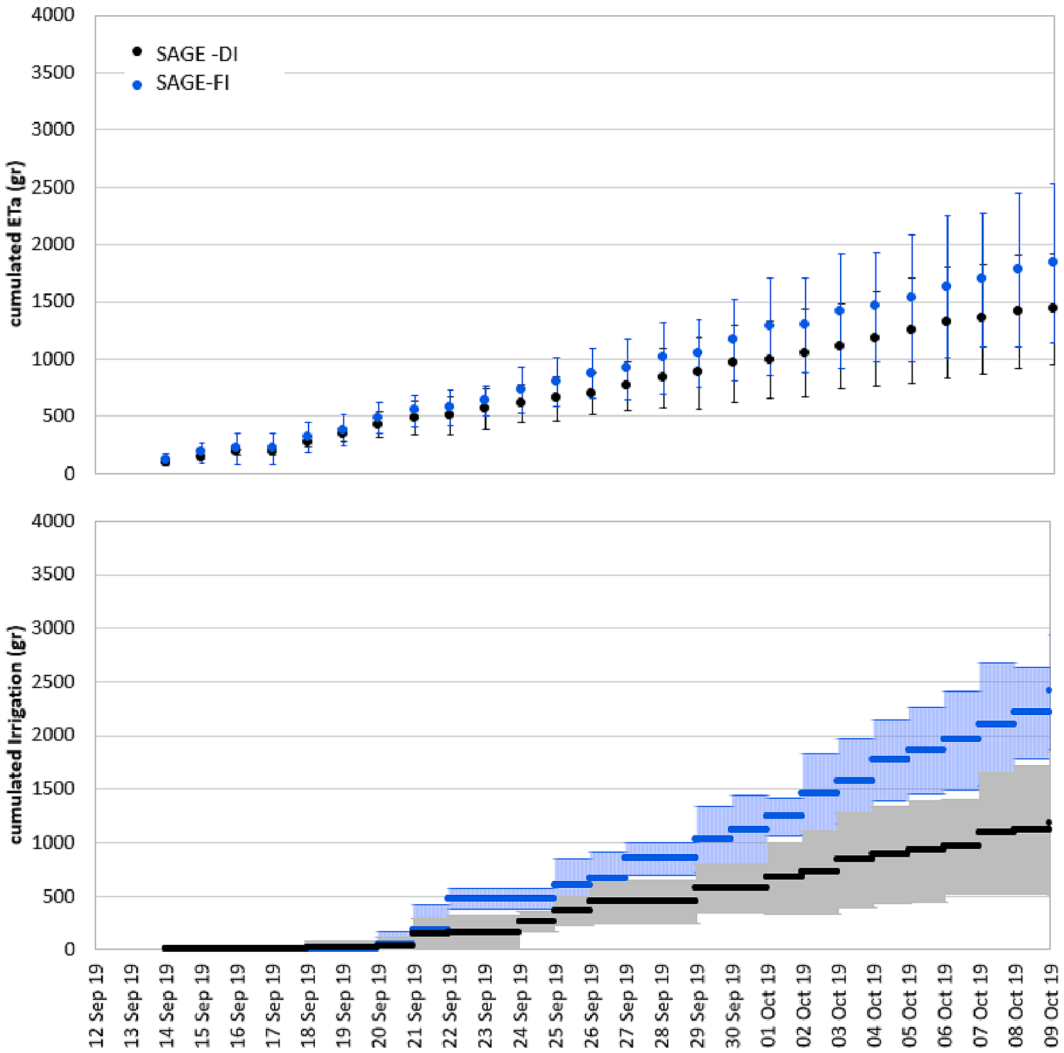

Fig. 10. Cumulative mean values and standard deviations of actual evapotranspiration (ET_a) and irrigation amount during the experimental period for the SAGE-FI and SAGE-DI treatments.

0.0001) between gravimetric-based daily ET_a and TDR-based *RWU* rates was obtained for the DI treatments. While a lower correlation (R^2 = 0.35, p-value < 0.0001) was found between the two methods for the FI treatments. The minor correlation on the FI could be explained by the fact that the TDR-based approach is not able to capture the variations of water status derived from the evaporation processes in the surface soil layers (i.e., first 5 cm depth), as the TDR metal rods were installed at the bottom of the pot and did not reach the first 5 cm of topsoil. Therefore, the TDR-based approach is not able to estimate the ET_a accurately when the irrigation volumes applied are more frequent and higher, which is translated into higher evaporation flux.

The frequency data distributions and the Shapiro-Wilk test depicted that the RWU data were non-normally distributed for either the FI or DI. On the other hand, the ET_a data was not normally distributed only for the DI treatment. Thus, the Mann-Whitney non-parametric test depicted that the TDR and gravimetric-based methods were statistically different in determining the water fluxes only in the FI treatment, which aligns with the lower correlation found in FI.

We could hypothesize that the TDR probes embedded within the pot are unaffected by the RWU gradients associated with the localized drip irrigation system and the spatial distribution of root density. Consequently, these methods would perform similar results to the gravimetric one when evaporation (*E*) is prevented. In a similar experiment, Halperin et al. (2017) evidenced a high correlation between the RWU and transpiration (T) variables on different tomato cultivars under FI and DI watering regimes. In this experiment, the measurement of only T was guaranteed by covering the exposed soil with plastic to stop the E fluxes.

Fig. 12 shows a screening of the agro-hydrological data obtained by plotting daily ET_a as a function of the soil water status (*FTSW*) and atmospheric evaporative demand (ET_0). The paired violins allowed detecting the differences in the data frequency distribution in terms of ET_a and *FTSW*. According to the Mann-Whitney test, the FI showed higher *FTSW* and ET_a values than the DI treatment.

A deeper analysis of the dataset showed the effect of the atmospheric demand, ET_0, on the crop evapotranspiration process, which was more marked for higher values of *FTSW*. On the contrary, for lower values of *FTSW*, the effect of ET_0 appeared more attenuated because the evapotranspiration fluxes are more dependent on soil water status. With a similar analysis, Halperin et al. (2017) demonstrated that solar radiation and vapor pressure deficit are the main forcings controlling the plant transpiration processes when soil water is not limiting.

Therefore, to describe the plant response to the soil water deficit conditions, it is necessary to use the relative evapotranspiration (*RET*) obtained by normalizing ET_a with ET_0.

To study the sensitivity of the indicators to the variations of the soil–plant water status, the values of *RET* and *FTSW* were correlated with midday stem water potential (*MSWP*) measurements and crop biometric characteristics, such as crop height (*H*). Fig. 13 shows the

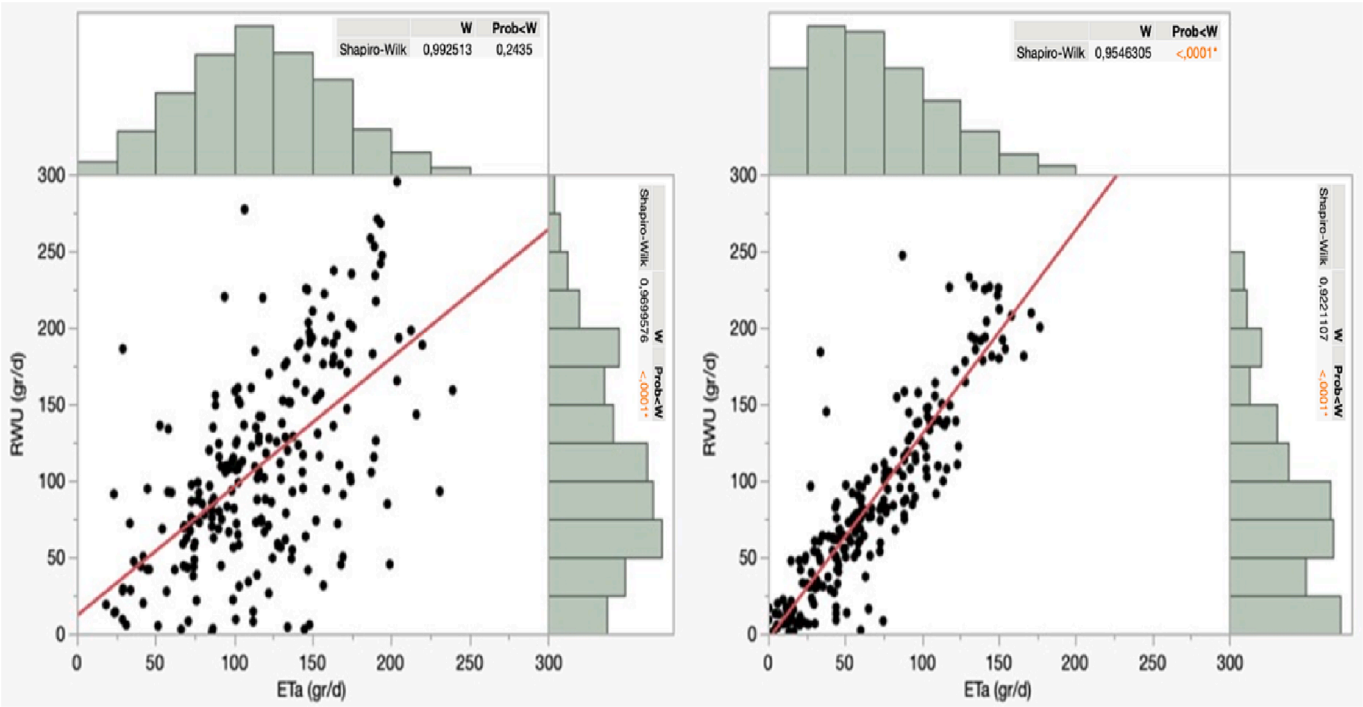

Fig. 11. Relationship between daily actual evapotranspiration (ET_a) and the root water uptake (RWU) for the full (a) and deficit irrigation treatments (b). The regression (red) line, the frequency distribution histograms and the Shapiro-Wilk goodness-of-fit test (for both variables) are also shown.

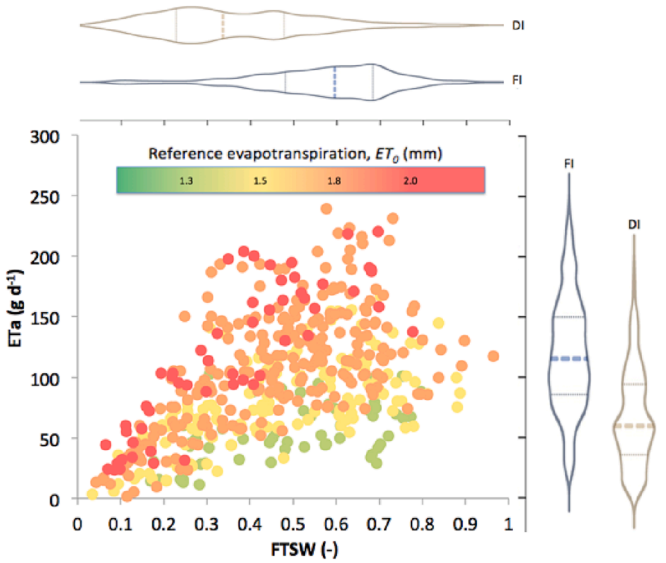

Fig. 12. Screening of the agro-hydrological data expressed as actual plant evapotranspiration (ET_a) versus soil water status (FTSW) and atmospheric evaporative demand (ET_0).

relationship between the average values of *MSWP*, *RET*, *FTSW*, and *H*. Each value reported in the plot is the average of four measurements acquired during the final period of the experiment.

There was a positive correlation between *RET* and *FTSW* with *MSWP*, indicating both indicators' ability to predict crop water status. Moreover, even the *H* was positively correlated with the indicators, as observed by the trend in the bubble colours. This screening suggested that the plant proxy data, such as *H* and thus its vigor, should always be accounted for in the soil–plant water relations because the plant vigor affects both the transpiration (higher vigour-higher transpiration) and evaporation (higher vigor-higher ground fraction cover-lower evaporation) processes.

The *RET* plateau depicted a range of the *MSWP* values between −0.6 and −0.8 MPa, which could indicate a domain of plant water status without stress, as demonstrated in Caser et al. (2018) and Mameli et al. (2011) respectively for *Salvia sinaloensis* (F.) and *Salvia officinalis* (L.).

Fig. 14 shows *RET* in response to the soil water status, quantified in terms of *FTSW*. The nonlinear regression analysis allowed to fit the logistic model (eq. (4) that was parameterized by fixing $a = 1$ and estimating the other two parameters, whose values resulted equal to $b = 8.93$ and $c = 8.57$ ($R^2 = 0.6$; p-value < 0.0001). The critical soil water status (*FTSW**), marking the transition to the water deficit condition, was determined as the intersection between the plateau and the tangent line through the curve's inflexion point.

This schematization suggests that at decreasing *FTSW*, the value of *RET* remains around the unit until a critical water status is reached (*FTSW**=0.52) and then falls in response to the lower soil water availability.

Halperin et al. (2017), using tomato (*Solanum pennelli* × *Solanum lycopersicum*), presented the relationship between plant transpiration and soil water content (θ). These authors showed that *T* was constant for a wide range of θ, then decreased linearly after a critical value of θ. The relationship proposed by these authors evidenced that θ represented a limiting factor for plant transpiration. In line with our results, nonlinear shapes of the water stress function were observed in previous research. Sadras and Milroy (1996), Sinclair (2005), and de Souza et al. (2014) evidenced a more realistic nonlinear relationship between the relative *T* response and soil drying, which was mathematically represented by a two-parameter logistic function.

A lower variability of the *RET* data was observed for *FTSW* < 0.52, compared to that characterizing the values of *FTSW* > 0.52, for which soil water status was not limiting plant transpiration. Consequently, the higher *RET* variability observed in the plateau of the curve could be linked to the atmospheric demand fluctuation since slight variations in the ET_o conditions would cause wider variances in the *RET* when soil water is not a limiting factor. On the other hand, the *RET* fluctuations would depend solely on the soil water content once the *FTSW** is

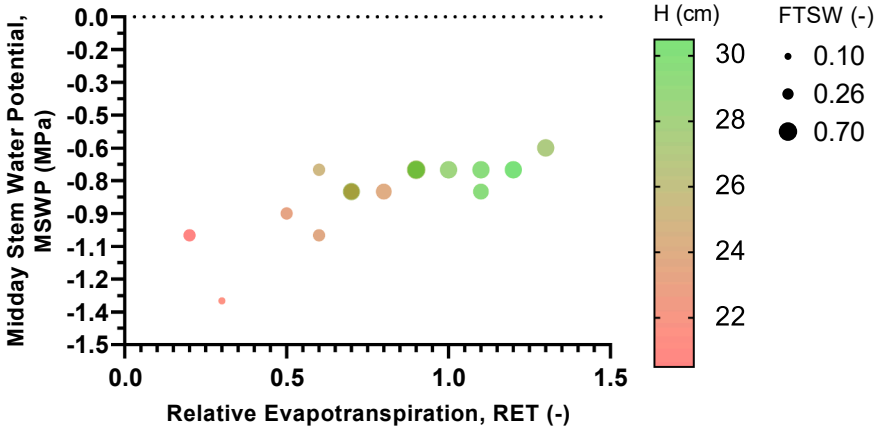

Fig. 13. Relationship between midday stem water potential (MSWP) and relative evapotranspiration (RET); the filling colours indicate the crop height (H) while the dot sizes the fraction of soil water available for transpiration (FTSW).

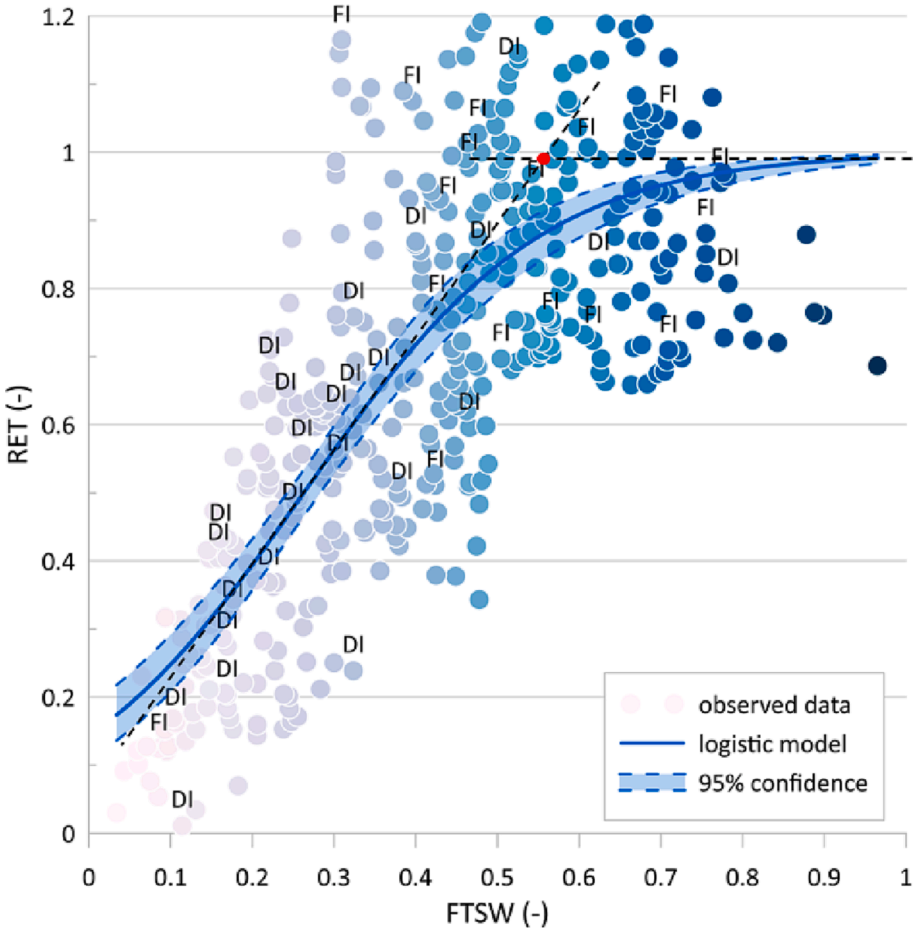

Fig. 14. Relative transpiration (RET) as a function of the fraction of soil water available for transpiration (FTSW); the root water uptake model expressed with a three-parameters logistic function with a 95% of confidence interval is also shown.

reached. In this case, the roots can compensate for the lower soil water content, thus reducing the *RET* variability.

This behavior was commonly described in other experiments using the macroscopic root water uptake modeling. For instance, de Souza et al. (2014) found that the variability of transpiration data of different potato cultivars was higher in the range of *FTSW* between 0.50 and 1.0. Mainly, other studies (Sinclair, 2005; de Souza et al., 2014) refer that the lower the air temperature, solar radiation, and VPD, the greater the variability of the *RET* data.

Moreover, Guswa (2004) attributed the *RET* variability observed at the lower *FTSW* values to the RWU gradient that would depend on the combined effect of the soil water content and root density.

In this case, the spatial distribution of the *RWD* allowed the plant to compensate for the effect due to the spatial variability of the lower soil water content. Thus, the roots located in the wetter soil volume can extract more water from the soil, compensating for the reduced activity of the roots found in the soil volume with lower water content, hence stabilizing the RET fluctuations (Guswa et al., 2004).

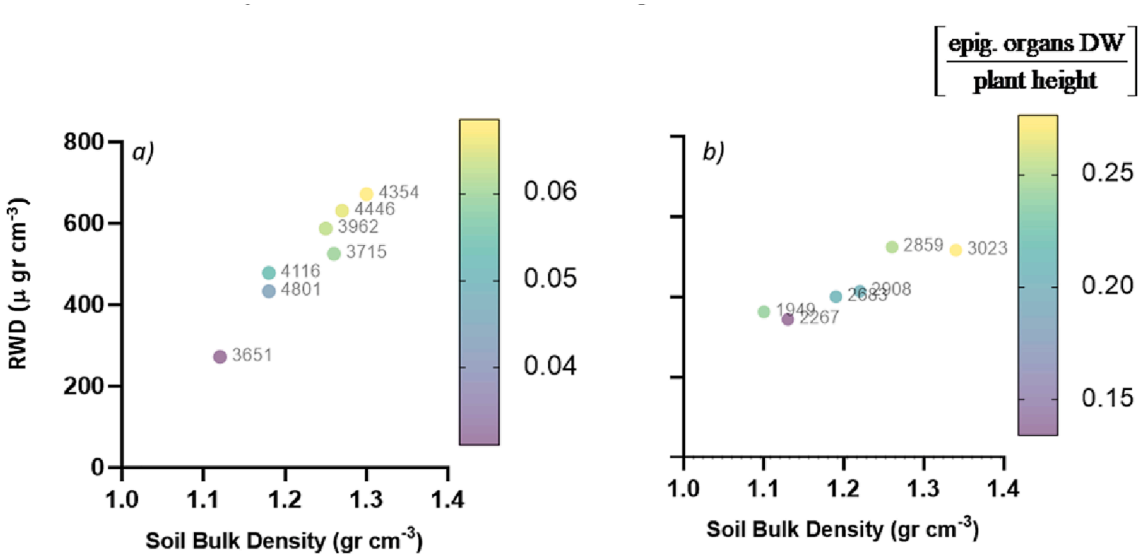

Fig. 15. Root weight density (RWD) as a function of soil bulk density for a) full and b) deficit irrigation treatments. The bubble colour gradients represent the ratio between the dry weight of the epigeal organs and the plant height, whereas the number close to the bubble is the cumulated ET_a expressed in grams (g).

3.4. Effect of soil bulk density (BD) on root water uptake (RWU)

The soil bulk density (*BD*) (g cm^{-3}) was variable (average: 1.22; standard deviation: ± 0.07; max: 1.34; min: 1.10) in both intra- and inter-treatments due to the non-homogeneous pot filling during the module preparation, and the continuous wetting/drying processes to which the soil was subjected. Fig. 15 shows the root weight density (*RWD*) for a unit of soil volume as a function of the *BD* for full and deficit irrigation treatments. In the same graph, the bubble colour gradients represent the ratio between the dry weight of the epigeal organs and the corresponding height (*H*). In contrast, the cumulated ET_a is reported close to the bubbles.

As observed, especially for the SAGE-FI treatment (Fig. 15a), BD strongly influences the amount of *RWD*. A similar positive trend is also visible in SAGE-DI treatment. Likewise, the amount of cumulative ET_a naturally increases with the root density and the corresponding epigeal part of the plant. The achieved results evidenced that *RWD* values tended to increase in the range of *BD* between 1.10 and 1.34 g cm^{-3}. This last result is confirmed by the literature aimed at assessing the effects of soil physical properties (i.e., *BD*) on the development of the surface root area (*SRA*). Lõhmus et al. (1989) presented a positive correlation between the *SRA* and the *BD* based on a quadratic function obtained for Norway spruce (*Picea abies*) for a range of *BD* like that investigated in this study.

Consequently, the homogeneous physical characteristics of the soil substrate in a controlled experiment are crucial to avoid side treatment effects on the HTS system implementation.

4. Conclusions

The current study presents a High-Throughput Screening (HTS) system that continuously measures plant responses to water deficit conditions. The system was designed by combining a pot weighing system with TDR-based soil moisture sensors, and it was placed in a greenhouse environment.

The application of the HTS system aimed i) to find the best mathematical schematization of the root water uptake (*RWU*), ii) to compare the gravimetric-based and the soil moisture-based approaches to measuring the ET_a fluxes, and iii) to analyze the effects of the soil bulk density variability on the measured *RWU* fluxes.

To test the system, full and deficit irrigation treatments were set using feedback control of irrigation scheduling to study the sage crop response to different water deficit conditions. The full irrigation treatment, as expected, evidenced generally higher soil water content (θ) and plant evapotranspiration (ET_a) than the deficit treatment. The large intra-treatment variability observed for the ET_a and irrigation amount could be related to each treatment plant's different root water uptake (RWU) intensity, due to the feed-back irrigation control, which was based on the soil water content threshold.

The relationship between the gravimetric-based daily ET_a and the TDR-based *RWU* rates showed a high correlation ($R^2 = 0.77$) in the DI treatment, while a lower R^2 ($R^2 = 0.33$) was depicted for the FI treatments. This fact could be explained by the inability of the TDR to detect the E fluxes in more frequent watering events. Even if the TDR probes are embedded in the pot to detect the whole plant RWU variability, they do not cover the first 5 cm of the soil substrate.

Apart from this, using the TDR probe embedded in the pot could enable uninterrupted and accurate tracking of the *RWU* over time, which, to the best of our knowledge, has not been tested quantitatively before in a HTS system.

The relative evapotranspiration (*RET*) and the fraction of soil water content available for plant transpiration (*FTSW*) resulted in being quite sensitive to the variations of the soil–plant water status. Both indicators positively correlated with midday stem water potential (*MSWP*). Moreover, the *RET* and *FTSW* were also correlated to plant height. Thus, the crop biophysical parameters can affect crop transpiration and soil evaporation, and they should be considered in the soil–plant water relations.

The *RWU* process was represented by a nonlinear (logistic) relationship between the *RET* and *FTSW*. This allowed identifying the critical threshold of *FTSW* defining the incipient occurrence of water deficit conditions for the sage crop. The *RET* values above the critical threshold of *FTSW* showed relatively higher variability than that beyond the threshold, evidencing the plant roots' ability to compensate for the spatial heterogeneity of soil moisture under higher soil water contents. Finally, the soil bulk density was positively correlated to the root weight density in the range between 1.10 and 1.34 g cm^{-3}, highlighting the importance of accomplishing accurately and homogeneously the pot filling to avoid possible effects due to the sample preparation.

Future research will involve replacing the small pots with larger containers to resemble filed conditions and quantify the effect of soil bulk density over the critical soil water status threshold, indicating quantifying the beginning of the leaf stomatal clousure.

CRediT authorship contribution statement

Àngela Puig-Sirera: Conceptualization, Methodology, Data curation, Writing – original draft. **Lorenzo Bonzi:** Investigation, Writing – review & editing. **Lorenzo Cotrozzi:** Investigation, Writing – review & editing. **Fatma Hamouda:** Investigation, Writing – review & editing. **Alessandra Marchica:** Investigation, Writing – review & editing. **Giuseppe Provenzano:** Writing – review & editing. **Damiano Remorini:** Writing – review & editing. **Giovanni Rallo:** Conceptualization, Methodology, Data curation, Writing – review & editing.

Declaration of Competing Interest

The authors declare that they have no known competing financial interests or personal relationships that could have appeared to influence the work reported in this paper.

Data availability

Data will be made available on request.

Acknowledgments

We thank Dr. A. Sbrana (University of Pisa) for providing support on the hardware and software development. The research was carried out in the frame of "Progetto OP-Illuminati Frutta-Rallo" (University of Pisa, 1048 MIPAF-Regione Toscana) and "ATMOSMART-dimostratore tecnologico" (University of Pisa)".

Appendix A. Supplementary material

Supplementary data to this article can be found online at https://doi.org/10.1016/j.compag.2023.107998.

References

Allen, R, Pereira, L, Raes, D., Smith, M., 1998. Crop evapotranspiration, a guideline for computing crop water requirements. FAO Irrigation and Drainage Paper No. 56, 2008th ed. FAO, Rome.

Ardakani, M.R., Abbaszadeh, B., Haghighi, M.L., 2014. The effect of drought stress on three clary sage (Salvia sclarea L.) populations from different habitats. J. Bio. & Env. Sci 5, 133–142.

Atkinson, J.A., Pound, M.P., Bennett, M.J., Wells, D.M., 2019. Uncovering the hidden half of plants using new advances in root phenotyping. Curr. Opinion in Biotechnol. 55, 1–8. https://doi.org/10.1016/j.copbio.2018.06.002.

Böhm, W., 1979. Container methods. In: Methods of Studying Root Systems. Ecological Studies. Springer, Berlin, Heidelberg. https://doi.org/10.1007/978-3-642-67282-8_10.

Caser, M., D'Angiolillo, F., Chitarra, W., Lovisolo, C., Ruffoni, B., Pistelli, L., Pistelli, L., Scariot, V., 2018. Ecophysiological and phytochemical responses of Salvia sinaloensis Fern. to drought stress. Plant Growth Regulation 84, 383–394. https://doi.org/10.1007/s10725-017-0349-1.

CR1000 Measurement and Control System. 2013 Campbell Scientific, Inc. Available on: https://s.campbellsci.com/documents/br/manuals/cr1000.pdf.

Dalal, A., Shenhar, I., Bourstein, R., Mayo, A., Grunwald, Y., Averbuch, N., Attia, Z., Wallach, R., Moshelion, M., 2020. A telemetric, gravimetric platform for real-time physiological phenotyping of plant–environment interactions. J. Vis. Exp. 2020, 1–28. https://doi.org/10.3791/61280.

de Souza, A.T., Streck, N.A., Heldwein, A.B., Bisognin, D.A., Winck, J.E.M., da Rocha, T. S.M., Zanon, A.J., 2014. Transpiration and leaf growth of potato clones in response to soil water deficit. Scientia Agricola 71, 96–104. https://doi.org/10.1590/S0103-90162014000200002.

Evett, S.R., Mazahrih, N.T., Jitan, M.A., Sawalha, M.H., Colaizzi, P.D., Ayars, J.E., 2009. A weighing lysimeter for crop water use determination in the Jordan Valley. Jordan. Trans. ASABE 52, 155–169.

Gosa, S.C., Lupo, Y., Moshelion, M., 2019. Quantitative and comparative analysis of whole-plant performance for functional physiological traits phenotyping: new tools to support pre-breeding and plant stress physiology studies. Plant Science 282, 49–59. https://doi.org/10.1016/j.plantsci.2018.05.008.

Guswa, A.J., Celia, M.A., Rodriguez-Iturbe, I., 2004. Effect of vertical resolution on predictions of transpiration in water-limited ecosystems. Adv. Water Res. 27, 467–480. https://doi.org/10.1016/j.advwatres.2004.03.001.

Halperin, O., Gebremedhin, A., Wallach, R., Moshelion, M., 2017. High-throughput physiological phenotyping and screening system for the characterization of plant-environment interactions. Plant J. 89, 839–850. https://doi.org/10.1111/tpj.13425.

IMCCP. 2011. Institute of Measurement and Control Code of Practice. A Code of Practice for the Calibration of Industrial Process Weighing Systems. ISBN 0 904457 23 0.

Jiménez-Carvajal, C., Ruiz-Peñalver, L., Vera-Repullo, J.A., Jiménez-Buendía, M., Antolino-Merino, A., Molina-Martínez, J.M., 2017. Weighing lysimetric system for the determination of the water balance during irrigation in potted plants. Agric. Water Manag. 183, 78–85. https://doi.org/10.1016/j.agwat.2016.10.006.

JMP® Version 17. SAS Institute Inc., Cary, NC, 1989–2023.

Joshi, D.C., Singh, V., Hunt, C., Mace, E., van Oosterom, E., Sulman, R., Jordan, D., Hammer, G., 2017. Development of a phenotyping platform for high throughput screening of nodal root angle in sorghum. Plant Methods 13, 1–12. https://doi.org/10.1186/s13007-017-0206-2.

Lõhmus, K., Oja, T., Lasn, R., 1989. Specific root area : a soil characteristic. Plant and Soil 119, 245–249.

Mameli, M.G., Zucca, L., Maxia, M., Manca, G., Satta, M., 2011. Effects of different irrigation management on biomass and essential oil production of Thymus vulgaris L., Salvia officinalis L., and Rosmarinus officinalis L., cultivated in the Southern Sardinian climate (Italy). Acta Horticulturae 889, 469–474. https://doi.org/10.17660/ActaHortic.2011.889.59.

Marchica, A., Loré, S., Cotrozzi, L., Lorenzini, G., Nali, C., Pellegrini, E., Remorini, D., 2019. Early detection of sage (*Salvia officinalis* L.) responses to ozone using reflectcance spectroscopy. Plants 8, 346.

Minjiao, L., Jeewantinie, K., Kaihotsu, I., 2015. A data-driven method to remove temperature effects in TDR-measured soil water content at a Mongolian site. Hydrological Res. Lett. 9, 8–13. https://doi.org/10.3178/hrl.9.8.

Negin, B., Moshelion, M., 2016. The advantages of functional phenotyping in pre-field screening for drought-tolerant crops. Functional Plant Biol. 44, 107–118. https://doi.org/10.1071/FP16156.

Pellegrino, A., Gozé, E., Lebon, E., Wery, J., 2006. A model-based diagnosis tool to evaluate the water stress experienced by grapevine in field sites. Eur. J. Agronomy 25 (1), 49–59.

Polak, A., Wallach, R., 2001. Analysis of soil moisture variations in an irrigated orchard root zone. Plant and Soil 233, 145–159. https://doi.org/10.1023/A:1010351101314.

Puig-Sirera, À., Provenzano, G., Gonz, P., Intrigliolo, D.S., Rallo, G., 2021. Irrigation water saving strategies in Citrus orchards : analysis of the combined effects of timing and severity of soil water deficit. Agricultural Water Manage. 248 https://doi.org/10.1016/j.agwat.2021.106773.

Rallo, G., González-Altozano, P., Manzano-Juárez, J., Provenzano, G., 2017. Using field measurements and FAO-56 model to assess the eco-physiological response of citrus orchards under regulated deficit irrigation. Agricultural Water Manage. 180, 136–147. https://doi.org/10.1016/j.agwat.2016.11.011.

Sadras, V.O., Milroy, S.P., 1996. Soil-water thresholds for the responses of leaf expansion and gas exchange: a review. Field Crops Res. 47, 253–266. https://doi.org/10.1016/0378-4290(96)00014-7.

Savitzky, A., Golay, M.J., 1964. Smoothing and differentiation of data by simplified least squares procedures. Anal. Chem. 36 (8), 1627–1639.

Sheskin D.J., 2007. Handbook of parametric and nonparametric statistical procedures, 4th edition.

Sinclair, T.R., 2005. Theoretical analysis of soil and plant traits influencing daily plant water flux on drying soils. Agronomy J. 97, 1148–1152. https://doi.org/10.2134/agronj2004.0286.

Sinclair, T.R., 2017. Early partial stomata closure with soil drying. In: Sinclair, T.R. (Ed.), Water-Conservation Traits to increase Crop Yields in Water-Deficit Environments. Case Studies. Springer, Raleigh, NC, USA, pp. 5–9.

Sinclair, T.R., Ludlow, M.M., 1986. Influence of soil water supply on the plant water balance of four tropical grain legumes. Australian J. Plant Physiol. 13, 329–341. https://doi.org/10.1071/PP9860329.

Stahl, A., Wittkop, B., Snowdon, R.J., 2020. High-resolution digital phenotyping of water uptake and transpiration efficiency. Trends in Plant Sci. 25, 429–433. https://doi.org/10.1016/j.tplants.2020.02.001.

Topp, G.C., Davis, J.L., Annan, A.P., 1980. Electromagnetic determination of soil water content: measurement in coaxial transmission lines. Water Resources Res. 16, 574–582.

Turner, M.T., Jarvis, G.P., 1982. Measurement of plant water status by the pressure chamber technique. Irrigation Sci. 9, 289–308.

Walter, A., Liebisch, F., Hund, A., 2015. Plant phenotyping: from bean weighing to image analysis. Plant Methods 11, 1–11. https://doi.org/10.1186/s13007-015-0056-.

Xu, P., Moshelion, M., Wu, X., Halperin, O., Wang, B., 2015. Natural variation and gene regulatory basis for the responses of asparagus beans to soil drought. Front. Plant Sci. 6, 1–14. https://doi.org/10.3389/fpls.2015.00891.